Title

Developmental staging and salinity tolerance in embryos of the delta smelt, Hypomesus transpacificus

Authors

Romney, Amie LT
Yanagitsuru, Yuzo R
Mundy, Paige C
et al.

Publication Date

2019-09-01

DOI

10.1016/j.aquaculture.2019.06.005

Peer reviewed

HHS Public Access

Author manuscript

Aquaculture. Author manuscript; available in PMC 2020 September 15.

Published in final edited form as:

Aquaculture. 2019 September 15; 511: . doi:10.1016/j.aquaculture.2019.06.005.

Developmental Staging and Salinity Tolerance in Embryos of the Delta Smelt, *Hypomesus transpacificus*

Amie L. T. Romney[1], **Yuzo R. Yanagitsuru**[2], **Paige C. Mundy**[1], **Nann A. Fangue**[2], **Tien-Chieh Hung**[3], **Susanne M. Brander**[4], **Richard E. Connon**[1,*]

[1]Department of Anatomy, Physiology, and Cell Biology, University of California, Davis, CA 95616, USA

[2]Department of Wildlife Conservation and Fish Biology, University of California, Davis, CA 95616, USA

[3]Fish Conservation Culture Laboratory, Department of Biological and Agricultural Engineering, University of California, Davis, CA 95616, USA

[4]Department of Environmental and Molecular Toxicology, Oregon State University, Corvallis, OR 97331, USA

Abstract

Delta smelt (*Hypomesus transpacificus*) is a critically endangered species endemic to the San Francisco Bay Delta (SFBD). Important for the conservation of this species is understanding the physiological and ecological impacts contributing to their population decline, and current studies lack information on embryonic development. Changes in patterns of salinity across the SFBD may be a particularly important environmental stressor contributing to the recruitment and survival of the species. Throughout their ontogeny, delta smelt may exhibit unique requirements and tolerances to environmental conditions including salinity. Here, we describe 22 stages of embryonic development of *H. transpacificus* that characterize early differentiation from the fertilized egg until hatching, allowing the identification of critical morphological features unique to this species. Additionally, we investigated aspects of physiological tolerance to environmental salinity during development. Embryos survived incubation at salinity treatments between 0.4 and 20 ppt, yet had lower hatch success at higher salinities. Prior to hatching, embryos exposed to higher salinities had increased osmolalities and reduced fractions of yolk implying that the elevated external salinity altered the physiology of the embryo and the environment internal to the chorion. Lastly, egg activation and fertilization appear to also be impacted by salinity. Altogether, we suggest that any potential tolerance to salinity during embryogenesis, a common feature in

*Corresponding author at: Department of Anatomy, Physiology, and Cell Biology, University of California, Davis, CA 95616, USA. reconnon@ucdavis.edu.

Author Contributions

ALTR, YRY, REC, and NAF conceptualized and designed the experiments. ALTR, YRY and PCM performed the experiments and analyzed the data. TCH oversaw the rearing of adult *H. transpacificus* and coordinated the provision of embryos. SMB provided initial input into the experimental design. ALTR drafted the initial manuscript with detailed edits from all authors. All authors reviewed and commented on the manuscript. The authors declare no competing interests.

euryhaline teleost species, impacts life cycle transitions into, and out of, embryonic development. Results from this investigation should improve conservation and management practices of this species and further expand our understanding of the intimate relationship between an embryo and its environment.

Keywords

Endangered fish; salinity tolerance; early life stage; chorion; egg activation

1. Introduction

Teleost embryos are largely prepared to contend with ecologically-relevant environmental stress. Their encapsulation within a chorion provides physical protection with selective permeability while physiological mechanisms to maintain homeostasis develop (Alderdice, 1988, Hamdoun et al., 2007). The embryo exists in states of morphology and physiology that are transient and unique to each developmental stage, and organismal survival depends on successful growth and maturation during critical developmental periods. Any disruptions in cellular division, migration or differentiation can impact not only the form of individuals, but functionality as well. How physiological impairment of embryonic development affects individuals across their life cycle is complicated to predict, as it is species-specific and may not manifest until later life history stages (Alderdice, 1988, Hamdoun and Epel, 2007, Krogh et al., 1937).

For an estuarine species such as the delta smelt (*Hypomesus trcmspacificus*), which inhabits areas with variable environmental salinity, understanding how salinity impacts proper development can provide practical information for future conservation aquaculture and management. The delta smelt is endemic to the SFBD, and since the mid 1990's, delta smelt abundance has rapidly declined and is now listed as critically endangered (Bennett, 2005). Delta smelt have a migratory annual life cycle where life stages vary both seasonally and spatially across the SFBD (Komoroske et al., 2014). During winter, the adults travel upstream to spawn in freshwater, and when larvae mature into juveniles during the late spring, they begin migrating downstream toward low salinities zones (1–6 ppt) where they remain until the next winter while continue to mature (Bennett, 2005). Adult *H. trcmspacificus* are euryhaline and largely remain in the upper SFBD between areas of fresh and brackish water (Komoroske et al., 2014, Wang, 2007). Salinity, among other abiotic conditions, is already being altered by climate change within the SFBD; with reductions in freshwater entering the estuary allowing for subsequent intrusions of higher salinity waters (Cloern et al., 2012, Moyle et al., 2010). Salinity appears to be a major determinant of where spawning and egg deposition occurs. Observations are uneven across life stages; gravid females and eggs have been reported from several freshwater sloughs (Lindberg et al., 1993) yet not until larval stages are individuals found downstream (Bennett, 2005). A critical assessment of the biology of these earliest life stages and the optimal conditions associated with spawning and successful reproduction is still missing from the broad literature on this species.

To further our understanding of the physiological tolerance to salinity during embryonic development of *H. transpacificus*, we established a detailed staging scheme of morphological differentiation independent of time. A common set of terms in coordination with those used for closely related teleosts provide the potential for comparative studies in the future. More so, stages among teleosts are predictably morphologically similar and largely conserved excluding traits of egg size and developmental timing (Richardson et al., 1997). A previous description of development has been reported for *H. transpacificus*, but with limited detail on morphology and without discrete developmental stages (Mager et al., 2003). This work aims to improve upon previous efforts by including a serial characterization of the differentiation of the fertilized egg into the functionally integrated larva. For future research, performing experiments in reference to stage rather than developmental time will increase the reproducibility of the experiment and more specifically elucidate processes impacted by environmental stressors. In fact, as a result of the dynamic physiological and morphological states of the organism between fertilization and hatching, experimental outcomes can be stage-specific.

In the current study, we described the embryonic development of *H. transpacificus* and tolerance to environmental salinity. We identified a staging series based on morphology that allows for the broader utility of this species for future investigations into physiological adaptations and knowledge required for conservation management. We also described salinity impacts by exploring features of embryogenesis such as growth and osmolality, as well as the transitions into and out of the embryonic period, including egg activation, fertilization, and hatching. With a deeper investigation of the embryo-environmental relationship, we contribute to the growing literature addressing the mechanisms for adaptation to salinity across the life history of this sensitive and endangered species.

2. Materials and methods

2.1. Broodstock and embryo collection

H. transpaciflcus embryos and eggs were obtained in 2018 via strip-spawning during the natural breeding season (February-May) from a genetically managed, 11th-generation refuge population maintained in freshwater (0.2 ppt) at 16°C (Baskerville-Bridges et al., 2005, Finger et al., 2018, Lindberg et al., 2013) by the Fish Conservation Culture Laboratory (FCCL), University of California, Davis (UCD). This refuge population has minimal loss of genetic diversity from wild populations and can be used to predict responses in naturally occurring delta smelt (Finger et al., 2018). For all investigations using fertilized eggs, excluding morphological description, crosses between no less than 3 male-female pairs were used to provide genetic diversity within clutches of offspring. Immediately after fertilization, adhesive embryos were treated with bentonite clay to prevent embryos from adhering to one another and to container surfaces. Embryos were then transferred from FCCL (Byron, CA) to UCD (Davis, CA), unless stated otherwise. Cohorts of embryos were housed in culture dishes within temperature-controlled incubators (16°C) and in the dark unless under observation. Embryo incubation media (see below) were changed every 24 hours (h) to maintain water quality. All handling, care and experimental procedures used were reviewed

and approved by the UCD Institutional Animal Care and Use Committee (IACUC Protocol # 20274).

2.2. Developmental staging

Embryos used to determine developmental staging were housed in culture dishes in freshwater (sterile-filtered with 0.2 μm pore size, 0.4 ppt, pH 8.2) at 16°C. Embryos were examined from fertilization to hatching under magnification using a Leica S8APO stereo microscope and photographed with a mounted 12-megapixel camera. Optionally, brightfield and differential interference contrast observations were performed to observe details of development in later stage embryos (Olympus LX71 inverted microscope, Tokyo, Japan). Images were collected, cropped, and edited for orientation using GNU Image Manipulation Program (GIMP 2.8.14). Multiple images were taken at an extended depth of field and a composite image was generated by image-stacking. Minor alterations to the brightness and contrast of images was used to achieve optimal exposure and contrast.

2.3. Actinomycin-D inhibition of development

Immediately after fertilization, embryos were transferred individually into the wells of 96-well plates with freshwater (0.4 ppt) and supplemented with concentrations of a transcriptase inhibitor, actinomycin-D (Sigma-Aldrich, St. Louis, MO), to examine the progression of development past the maternal-to-zygotic transition (MZT; Lee et al., 2014). Embryos that do not initiate genomic transcription in response to the inhibitor cannot transition morphological and in result can stall in development, allowing for the identification of which stage the MZT in this species (Podrabsky et al., 2017, Zamir et al., 1997). The final concentration of dimethyl sulfoxide (DMSO) was 1.0% v/v with 50, 100, 200, and 400 μM concentrations of actinomycin-D. An additional control group was included with 1.0% DMSO without the inhibitor. The morphological progression of actinomycin-D-treated embryos was compared to embryos under control conditions: freshwater and freshwater + 1.0% DMSO (n = 36 per treatment). Embryos were monitored and staged morphologically over a period of 50 h and the remaining individuals that survived treatments were also recorded.

2.4. Salinity dependent embryonic survival and hatching

A total of 3,500 embryos were prescreened under a dissecting microscope to remove nonviable eggs (determined by loss of translucency and chorion intactness). Living embryos were divided into replicate culture dishes of freshwater (0.4 ppt). Embryo incubation media included freshwater (0.4 ppt, pH 8.2) and salinity treatment solutions (2.0, 4.0, 8.0, 10.0, 16.0, and 20.0 ppt; Swanson, 1996, Machado and Podrabsky, 2007). All treatment solutions were prepared using Red Sea Coral Pro salt mix (Red Sea Houston, TX, USA), confirmed for salinity using a YSI water quality and conductivity meter (YSI Incorporated, Yellow Springs, OH, USA), and sterile-filtered (0.2 μm). Salinity was adjusted to treatment concentrations gradually at a rate of 2 ppt $\cdot$ h^{-1}. Embryos were incubated without aeration (water was changed daily) or light exposure for the duration of development. Percent survival was determined for all dishes (n= 5 per salinity) every 24 h under low light conditions using a dissecting microscope. Non-viable embryos were removed daily so not to influence hatching measurements. Once embryos began hatching, the number of larvae per

culture dish was recorded in addition to embryo survival in order to determine hatch timing in each salinity treatment. Once all embryos had hatched or perished in a culture dish, hatch success was calculated by dividing the total number of larvae that hatched by the number of embryos that were in the dish at the start of the experiment.

2.5. Morphometrics and intrachorionic osmolality

For each salinity treatment, five groups of 75 embryos at seven days post-fertilization (dpf) were rinsed by pipetting embryos gently up and down in 1 mL for 1 minute of ultrapure water to remove residual salts on their chorion surfaces from the treatment solutions (adapted from Machado and Podrabsky, 2007). Water was drained from embryos by placing them on a 100 μm nylon mesh screen and rinsed again with 1 mL of filtered water. Runoff water was wicked away and embryos were then gently patted dry and homogenized in a microcentrifuge tube before being centrifuged at 6,000 rpm for approximately 2 minutes. Immediately following centrifugation, 10 μL of supernatant were drawn and used for measuring osmolality using a VAPRO 5600 vapor pressure osmometer (WesCor Inc, Logan, UT; Machado and Podrabsky, 2007). The osmolality of each treatment solution was also measured.

Embryos at stage 21 (7 dpf) which coincides with the onset of cardiac contractions, were further examined and photographed under a stereomicroscope and measured using the imaging analysis software, ImageJ (National Institutes of Health, Bethesda, MD, USA) for morphometric analyses (Swanson, 1996). An electron microscopy grid was photographed throughout the observations in order to convert pixels to μm. Egg and yolk were modeled as spheroids and their volumes were calculated as: $4/3\pi \cdot x^2 y$, with x as the semi-major and y as the semi-minor axis.

2.6. Salinity dependent egg activation and fertilization

Eggs from three gravid females were stripped into a single dry collection tray and mixed together for homogeneity. Groups of 50 to 100 embryos were divided into four salinity treatments selected from the previous experiments: 0.0, 2.0, 4.0, and 8.0 ppt. Upon addition of treatment solutions to each dish (n = 3 per salinity), embryos were photographed with a microscope mounted with a Leica DFC420 camera (Leica M165C, Leica Microsystems Inc., Buffalo Grove, IL) for later measurements of perivitelline space expansion (Sørensen et al., 2016). Embryos were photographed every 20 min for 120 min. Photographs were measured using ImageJ. Perivitelline space was calculated as the difference in egg and yolk volume.

Fertilization experiments followed the same design as activation experiments. However, after collecting eggs into dry treatment dishes as mentioned above, sperm from three males was applied to each plate of eggs and gently stirred. Solutions of treatment salinities were added to the dishes of gametes and allowed to activate for 5 min. After this, solutions were replaced in each plate and continued to incubate at 16°C for 24 h to allow sufficient time for morphological determination of fertilization and progression through development as a measure of fertilization.

2.7. Statistical analysis

Interactions between percent survival and egg activation were compared between salinity treatments using a repeated measures, one-way analysis of variance (ANOVA) and post-hoc Tukey's pairwise method HSD test at each time point. Potential interactions between hatching, osmolality, yolk volume, egg volume, yolk fraction (yolk volume normalized to egg volume), and fertilization with treatment salinity were tested using a one-way ANOVA (Tukey's pair-wise method). We additionally analyzed the relationship between intrachorionic osmolality, and yolk fraction with salinity using simple linear regression. All statistical analyses were based on $\alpha = 0.05$ and were performed using GraphPad Prism (Version 7.0c, GraphPad Software, La Jolla California USA). All measurements are reported as the mean ± the standard error of the mean (SEM) unless otherwise stated.

3. Results

3.1. Developmental staging

Under laboratory conditions, (16°C, 0.4 ppt, no light), the duration of embryonic development was 10 days (Table 1). Eggs from a single brood at those conditions were synchronous in development and hatched within the same day. Embryonic development of *H. transpaciflcus* is characterized by 22 distinct morphological stages that span from fertilization to hatching based on the present observations and supported by descriptions previously made for this species and others (Kimmel et al., 1995, Mager, Doroshov, Van Eenennaam and Brown, 2003). Each stage is further labeled by more broadly describing periods of development including pre-fertilization, zygote, cleavage, blastula, gastrula, segmentation, pharyngula, and larvae. Each developmental stage is named and numbered (0-22) as shown below in a scheme that can be used comparatively with morphological stages for other teleost species.

3.1.1. Pre-fertilization period—Stage 0, Unfertilized egg (un-activated): Upon extrusion from the female and prior to any activation marked by the expansion of the perivitelline envelope, eggs were 0.94 ± 0.01 mm in diameter. The chorion is immediately adjoined to the plasma membrane surrounding the yolk mass which appears homogenous and granular. Adhesion of the chorion to any substrate was observed immediately upon exposure to the external aqueous environment.

3.1.2. Zygote period—Stage 1, Activated/Fertilized: Perivitelline envelope separates away from the yolk mass ultimately forming the perivitelline space. Nonyolky cytoplasm relocates to what will become the animal pole, forming the blastodisc on surface of the yolk (Figure 1A). After complete expansion of the perivitelline space was confirmed (2 h), embryos were 1.01 ± 0.007 mm in diameter. Lipid droplets begin to coalesce within the yolk mass.

Stage 2, One cell: One cell (blastomere) is fully expanded from the yolk surface (Figure 1B). The cleavage furrow between the blastomere and yolk is shallow and the edges are flush with one another. Lipid droplets within the yolk mass continue to coalesce.

3.1.3. Cleavage period—Stage 3, Two cells: First cell division has taken place and two progeny or daughter cells of equal size can be seen with a deep cleavage furrow (Figure 1C). The cleavage is vertically oriented to the plane of the blastodisc (region of active cell division) formation. Cleavage appears meroblastic with the large yolk mass remaining localized at the vegetal pole.

Stage 4, Four cells: The second cell division has taken place at a plane perpendicular to the previous cleavage resulting in four daughter cells arranged in a 2 × 2 array (Figure 1D). All cells are along one horizontal row or tier and are in contact with the yolk.

Stage 5, Eight cells: The third cell division has taken place parallel to the first division at two separate cleavage planes creating a 2 × 4 array of blastomeres (Figure 1E). All cells continue to be in contact with the yolk along one tier when observed from the “face” view as describe previously (Kimmel, Ballard, Kimmel, Ullmann and Schilling, 1995).

Stage 6, Sixteen cells: The fourth cell division occurs perpendicular to the previous plane and blastomeres are in a 4 × 4 array (Figure 1F). Central four blastomeres are completely surrounded by the peripherally located marginal cells.

Stage 7, Thirty-two cells: Two tiers of blastomeres occur when viewed from the face of the embryo that curve around the animal pole, a lower one in contact with yolk, and an upper that is not (Figure 18). The orientation of cleavage plains become more oblique to one another.

Stage 8, Sixty-four cells: Cells along three tiers from the face view have a polygonal shape. Some are in contact with the yolk while others are in contact with only other blastomeres (Figure 1H). The latter are completely buried within other cells and are referred to as the deep cells.

Stage 9, 128 cells: The cluster of blastomeres begin taking on a taller ball-like appearance as it expands further towards the animal pole with five tiers of cells, the solid mound has a curved interface with the yolk surface underneath (Figure 1I).

3.1.4. Blastulaperiod—Stage 10, High Blastula: Counting the number of tiers of cells becomes increasingly difficult after the 256 cell stage corresponding to seven tiers of cells as the cleavage planes become less regularly arranged and difficult to distinguish from one another. This increases over time to 11 tiers for the 1,000 cell stage. The mound is taller and therefore is referred to as the “high”‘ blastula. From the face view including the yolk mass, the shape is more oblong or ellipsoidal (Figure 1J). The blastula develops a smooth outline as cellular cleavage become indeterminant. The circumference of the interface between blastomeres and yolk is slightly constricted.

Stage 11, Low/Flat Blastula: The mound of cells lowers in height; the animal-vegetal axis shortens, so that when including the yolk mass, the entire structure is more circular shaped likely in coordination with a reduction of the constriction around the blastula margin (Figure 1K). The interface between the yolk and blastula is flat.

3.1.5. Gastrula period—Stage 12, Early Epiboly: Epiboly commences when the interface between the blastula and the yolk begins to curve inward toward the animal pole and a curved band or thickening around the periphery of the blastula can be identified, consisting of many small blastomeres (Figure 1L). The blastula begins to expand around the yolk toward the vegetal pole. This continues until the periphery of the blastula, now the blastoderm, encompasses 30% of the yolk mass surface (Figure 1M).

Stage 13, Mid-Epiboly: The blastoderm expands to 50% of the yolk surface between the animal and vegetal poles (Figure 1N). At the marginal regions of the blastoderm, thickening results, forming the first evidence of the embryonic shield. The margin of the blastoderm advances to encompassing approximately 75% of the yolk mass surface.

Stage 14, Late Epiboly: The margin of the blastoderm continues to expand from 75 to 90% of the surface of the yolk mass (Figure 1O). The blastoderm continues to expand around the yolk until surrounding the yolk mass completely; 100% (Figure 1P). Sometimes, a small plug of yolk can be observed protruding from the zone of constriction as the blastoderm approaches closure at the vegetal pole.

Stage 15, Bud: Dorsal thickening is observed as the early embryonic body makes a C-shape protrusion reaching between the animal and vegetal pole (Figure 1Q). The thickened region of the animal pole will become the head and the region near the vegetal pole will become the tail.

3.1.6. Segmentation period—Stage 16, Early somite: The bud continues to encircle 50% of the yolk mass from the animal to the vegetal pole (Figure 1R). The thickened early embryonic body becomes distinguishable at either end; the thickening at the animal pole becomes more prominent as the prospective head region with bilaterally formed oval shaped eye cups, or optic placodes. At the vegetal pole, the tail bud only slightly thickens in comparison. Somitogenesis commences along the center of the anterior-posterior axis of the body with the first and second pair of somites barely visible by their somatic furrows. Each additional pair becomes more apparent and is better visualized with differential interference contrast. The head continues to thicken as the neural keel begins to form. The embryonic body continues to lengthen around the periphery of the yolk as somites continue to form reaching 10 pairs.

Stage 17, Mid-somite: Somitogenesis continues from 10 to 29 pairs of somites (Figure 1S). The optic placodes form into vesicles each with a lens placode (Supplemental Figure 1A). The head continues to grow taller and wider. Bilateral otic placodes can be observed posterior to the position of the hindbrain and over time, hollows out forming the otic vesicle. At the tail bud, the epithelial sac known as the Kupffer’s vesicle is noticeable. The body encircles 50% to 75% of the yolk. Melanocytes can be observed around the surface of the yolk mass.

Stage 18, Late somite: Somitogenesis increases from 30 to 45 pairs along the body axis and somites take on a chevron shape from the lateral view (Figure 1T). The body encircles 75% to 100% of the yolk from head to tail bud. Subdivisions of the developing brain appear with

the components of the forebrain, the telencephalon and diencephalon, which only subtly distinguishable central to the optic vesicles (Supplemental Figure 1B). The midbrain and the hindbrain, and the cerebellar primordium that separates them, can be seen posterior to the optic vesicles. The tail bud begins to grow off of the surface of the yolk. As it lengthens, the tail can often be positioned just slightly to the either side of the body axis.

3.1.7. Pharyngula period—Stage 19, Early embryo: The yolk is fully encircled by the embryo and the tail continues to lengthen, overlapping the head and reaching a position between the optic vesicles and otic vesicles (Figure 2A). There are between 45 and 55 pairs of somites. Eyes begin to pigment to a light grey color and continue to darken from the periphery inward toward the center. The heart begins to contract slowly. The first body movements appear as side to side contractions. Otoliths can be observed inside the otic vesicle (Supplemental Figure 1C). Primordial brain folds remain and are easily seen. However, the enclosed nervous system can be identified by the presence of a ventricle forming in the midbrain.

Stage 20, Mid-embryo: Eyes darken to a charcoal grey color evenly across the surface excluding the lens (Figure 2B; Supplemental Figure 1D). The tail lengthens past the position of the otoliths. Somites become difficult to identify and (> 55 pairs). Cardiac contractions and the frequency of body movements increases.

Stage 21, Late-embryo: The embryo has fully black-pigmented eyes with a translucent lens protruding outward (Figure 2C). Subtle eye movements can be observed. The head thickens and the axis appears to lift away from the surface of the yolk anteriorly, so that the lower jaw can be observed. The tail has twice encircled the yolk mass, now showing resemblance to a yolk sac. The embryo has the ability to reposition itself within the chorion with high speed and frequency. The degree of morphological change slows at this stage.

Stage 22, Yolk-sac larvae: Embryonic development is terminated as the embryo hatches out by breaking free through the chorion (Figure 2D). The released larva is translucent with a total body length between 4.3-5.6 mm (5.3 ± 0.1 mm). The yolk sac from the lateral view is ellipsoidal in shape. Translucent myotomes can be seen spanning anterior-posteriorly on the trunk of the body. The mouth is underdeveloped with the lower jaw unobservable in comparison to the upper jaw. The chorion continues to remain adhered to the substrate for multiple days after hatching.

3.2. Actinomycin-D inhibition of development

In *H. transpacificus*, embryos without any exposure to the transcriptase inhibitor, actinomycin-D developed continuously through stages of epiboly with a total survival rate of 97% and 86% under control conditions with 1.0% DMSO and without, respectively (Figure 3). Embryos maintained under increasing concentrations of the inhibitor showed a stall in developmental shortly after the high blastula (stage 11). After two days of observations, embryos with blastoderms that did not migrate around the yolk had an increased incidence of death with total survival rates at 86%, 58%, 30%, and 8% for 50, 100, 200, and 400 μM actinomycin-D, respectively.

3.3. Salinity dependent embryonic survival and hatching

The average embryo count per culture dish started at day 0.5 with 109 embryos ± 3 embryos. All treatments experienced mortality within 2.5 dpf. Average survival remained constant at 80% throughout the remainder of development with 77 ± 3%, 80 ± 3%, 81 ± 1%, 77 ± 2%, 78 ± 3%, 78 ± 3% for 0.4, 2.0, 4.0, 8.0, 10.0, 16.0, and 20.0 ppt, respectively, and showed no difference between salinities (for repeated measures ANOVA between treatments at all time points, $P > 0.05$).

Most embryos hatched by 10.5 dpf at salinities of 0.4, 2.0, and 4.0 ppt (86 ± 3%, 85 ± 4%, 92 ± 2%, respectively; Figure 4B). There was a significant reduction in hatching at 8.0 and 10.0 ppt (67 ± 6%, and 75 ± 3%, respectively; $F_{6,28} = 159.6$, $P < 0.0001$) and no hatching at 16.0 and 20.0 ppt. Embryos across treatment groups, excluding 20.0 ppt, continued to hatch until 12.5 dpf. By 12.5 dpf, cumulative percent hatching at 0.4, 2.0, 4.0, 8.0, and 10.0 ppt (97.8 ± 0.5%, 97.6 ± 0.7%, 98.0 ± 0.8%, 98.6 ± 1.3%, 93.4 ± 1.2%, respectively) was significantly higher than 16.0 and 20.0 ppt (15.8 ± 2.6%, 0%, respectively; $F_{6,28} = 1171$, $P < 0.0001$).

3.4. Intrachorionic osmolality and morphometrics of pre-hatch embryos

There were no differences in intrachorionic osmolality between 7 dpf embryos reared between 0.4 and 16.0 ppt, however osmolality at 20.0 ppt was significantly higher than that of 0.4, 2.0, 4.0 and 8.0 ppt treatments ($F_{6,31} = 9.37$ $P < 0.0001$; Figure 5A). Linear regression analysis showed a positive correlation of the intrachorionic osmolality with increasing salinity ($r^2 = 0.535$, $P < 0.001$).

Egg volume was not significantly different among treatment salinities ($F_{6,133} = 0.6693$, $P = 0.6746$; Supplemental Figure 2A). However, yolk volume showed significant differences between lower and higher salinities ($F_{6,133} = 6.799$, $P < 0.0001$; Supplemental Figure 2B). The yolk fraction between 0.4 and 2.0 ppt salinity treatments differed from 16.0 and 20.0 ppt conditions ($F_{6,133} = 5.317$, $P < 0.0001$). Linear regression analysis showed a negative correlation of yolk fraction with increasing salinity ($r^2 = .1646$, $P < 0.001$, Figure 5B).

Seven dpf embryos demonstrated unique physical characteristics at the chorion in result of treatment salinity (Figure 5C). Chorions of embryos at low treatment salinities (0.4 – 10.0 ppt) were soft and translucent as normal under microscopy. Chorions of embryos at 16.0 and even more so at 20.0 ppt were more rigid and opaque.

3.5. Salinity dependent egg activation and fertilization

Upon immediate exposure to their aqueous environment and without sperm present, eggs of *H. transpaciflcus* undergo activation exhibited by an expansion in space between the egg chorion and yolk mass (Figure 6A). Under all conditions, eggs expanded from a diameter of 0.94 ± 0.01 mm to 1.01 ± 6.7 mm, with corresponding volumes of $6.5 \times 10^7 \pm 0.1 \times 10^7$ μm^3 to $2.2 \times 10^8 \pm 0.06 \times 10^8$ μm^3 after 1 h. However, after twenty min the expansion of perivitelline space was greater in conditions of lower salinities; measurements at all salinities were significantly different from one another ($F_{3,36} = 5.349$, $P = 0.0038$) excluding the comparison between 4.0 and 8.0 ppt ($P = 0.9277$). After 40 min, the volume of

perivitelline space in embryos at 0.4 ppt remained significantly greater than the volume at 4.0 and 8.0 ppt ($P < 0.05$). When eggs were incubated in the same salinity concentrations (0.4, 4, 8, and 8 ppt), however in the presence of sperm, more eggs were successfully fertilized at 0.4 ppt (41 ± 8.9%) than eggs at 4.0 and 8.0 ppt (23 ± 3.8% and 25 ± 3.4%, respectively) however the differences were nonsignificant ($P > 0.05$ for all tests).

4. Discussion

We report a 22 stage embryonic morphological staging scheme from fertilization until hatching for *H. trcmspacificus* that greatly improves the resolution of previous developmental staging schemes (Mager et al., 2003, Wang, 2007). The stages defined here are in agreement with previous reports; however distinct morphological stages allowed for the detailed descriptions of the brain, eyes, and otoliths. Other comparative developmental descriptions for smelt species include the arctic rainbow smelt, *Osmerus eperlanus mordax*, (Takahashi et al., 2016) the pond smelt, *Hypomesus olidus* (Yamada, 1963) long-finned smelt, *Spirinchus lanceolatus* (Hikita, 1958) and the Kyuriuo, *Osmerus eperlanus mordax* (Yanagawa, 1978).

By inhibiting the onset of RNA transcription in early embryos, we found that *H. trcinspacificus* ceases to progress past the high blastula, marking this stage as the midblastula transition for this species; a time point that is similar to that of other species (Kane et al., 1993, Podrabsky et al., 2017). In all vertebrates, maternal factors are essential for coordinating the earliest stages of embryonic development (Abrams et al., 2009, Lindeman et al., 2010). The genetic regulation of development is initially provided by the maternal genome in the form of packaged RNA and protein (Baroux et al., 2008). Upon fertilization, the newly formed zygotic genome is transcriptionally inactive and completely relies on what is provisioned within the oocyte prior to ovulation. Not until later stages of development does the zygotic genome initiate its own transcription, and in coordinated fashion, silence the remaining factors provided maternally known as the MZT (Aanes et al., 2011). Genome activation has been identified to occur at the midblastula transition in zebrafish and it is a critical mechanism underlying aspects of maternal inheritance (Kane and Kimmel, 1993). For future work using this species, gene expression before or after this critical transition will represent distinct maternal and embryonic genome activity, respectively.

Embryos of *H. transpacificus* are capable of surviving and developing across a wide distribution of salinities (0.4 – 20.0 ppt), yet they require conditions lower than 16.0 ppt to hatch successfully. Survival throughout development highlights a tolerance to salinity at this stage, a common feature in euryhaline teleosts (Alderdice, 1988). In addition to effects of salinity on hatch success, we found that intrachorionic osmolality increased at higher salinities. This may suggest that embryos reared at higher salinities must expend more energy to cope with increased osmotic stress (Machado and Podrabsky, 2007). This is reflected in the reduced yolk fraction measured at higher salinities. Because newly hatched yolk-sac larvae depend solely on their yolk to sustain them with nourishment until 4 days post-hatch, when jaws develop and they can begin exogenous feeding (Baskerville-Bridges, Lindberg and Doroshov, 2005), individuals that were reared at higher salinities as embryos

may be disadvantaged with a reduced energetic budget for growth and development as early larvae.

The chorion was physically altered by salinity treatment and those at higher salinities became hardened and more opaque. These changes could potentially influence chorion permeability and are likely to prevent successful hatching. The chorion is largely perceived to function as a mechanism to protect the susceptible embryo from environmental conditions that cannot be tolerated. Yet chorions of pelagic fish have a structure and function that are also adapted to their environments and thus likely have limitations to their performance (Brivio et al., 1991, Potts et al., 1969). In general, and especially during early development, embryos of teleost are known to have minimal permeability to water and ions (Hagedorn et al., 1998, Krogh and Ussing, 1937). Despite the low permeability to ions and water, most freshwater fish embryos lack a high tolerance to increased environmental salinity (Mangor-Jensen et al., 1993). During embryogenesis for other teleosts, the permeability traits of the chorion are closely linked to other aspects including buoyancy and development of the yolk sac. How environmental salinity impacts these specific properties of developing *H. transpacificus* has yet to be investigated.

Interestingly, a feature identified among smelt species of the SFBD is chorion adhesion (Wang, 2007). A number of teleost species are known to deposit their eggs on substrates with this adhesive outer chorion layer (Hikita, 1958, Riehl et al., 1998, Rizzo et al., 2002, Brander et al., 2016). By doing so, embryos are localized to specific locations which may provide optimal environmental conditions for the particular species (Riehl, 1996). Upon exposure to the aqueous environment external to the female, the outer layer of the chorion, the external zona radiata, hydrates and becomes adhesive (Rizzo, Sato, Barreto and Godinho, 2002). Previous work has identified that under the influence of water the hydration of the fine outer layer, made mostly of glycoproteins, provides the chorion with adhesiveness (Cherr et al., 1982, Cherr et al., 1984). While it is likely that in *H. transpacificus* the adhesive chorions assists with localizing the eggs at a spawning site within the SFBD, characteristics regarding the substrate type, the ecological relationship with salt and water balance, as well as the association with fertilization has yet to be described.

Transitioning from an embryo to a yolk-sac larva upon hatching is physiologically challenging as it marks the initial exposure to the immediate environment (Alderdice, 1988, Hamdoun and Epel, 2007). It provides an opportunity to examine the physiology of a species with the perspective of metamorphosis between stages rather than at a singular life history stage. One of the major components of vertebrate development is the activation of the egg prior to fertilization (Epel, 1990). This process reintroduces the oocyte into the cellular cycle and prepares the oocyte physically and chemically for fertilization (Gilkey et al., 1978). Associated with this is the expansion of the perivitelline membrane from the yolk. Activation is coupled with fertilization and can often be induced by, or else facilitate, the successful entry of sperm (Lee et al., 1999, Pelegri, 2003). We found that egg activation in *H. transpacificus* embryos occurred more rapidly at lower salinities compared to higher salinities. Even though embryos from all treatments reached a similar maximum perivitelline space after 1 h, The initial rates of expansion may indicate a time window associated with egg viability and proper egg fertilization. While not statistically significantly different

between treatments, fertilization rates decreased as salinity increased. If an accelerated rate of activation occurs at lower salinities, a potential shift or extension may result in the timing of any such critical window for optimal rates of fertilization in *H. transpacificus*. Implications of the immediate impacts of elevated salinity on *H. transpacificus* eggs, after extrusion or ovulation, is critical. Further investigations on the chemical nature that specifically acts as the activation stimulus for this species should be pursued.

In conclusion, our work provides a detailed examination of the biology of *H. transpacificus* during embryonic development and life cycle transitions in the context of environmental salinity. A deeper understanding of the physiological adaptation of any species is best supported by investigations across all life stages on individual survival as well as the physical and biochemical properties that underlie any mechanisms of tolerance. Previous work on salinity tolerance during larval stages (Komoroske et al., 2014) and adults (Hasenbein et al., 2013) in combination with the present study can help achieve a more complete understanding of the physiological relationship between *H. transpacificus* and salinity. It is reasonable that the current data from a refuge population can be used to predict developmental outcomes in naturally anadromous wild populations of Delta smelt. The refuge population was founded in 2006 with 2300 wild-caught Delta smelt, nonetheless, after nine years of culture, microsatellite analyses indicated a minimal loss of genetic diversity and only small amounts of differentiation between the wild and refuge populations (Finger et al., 2018).

With current climate patterns of their habitat becoming increasingly unfavorable, and their potential for extinction, it is important to resolve such an interaction between animal and environment (Bennett, 2005, Hobbs et al., 2017). Any future investigations of *H. transpacificus* call for integrative approaches of life history, physiology, and ecology, in order to improve our understanding as well as conservation management efforts for this sensitive species.

5. Conclusions

Here we describe embryogenesis and tolerance to environmental salinity of *H. transpacificus*, a species undergoing a dramatic population decline as a result of anthropogenic impacts on its ecosystem. These stages can serve as a useful metric independent of time, a factor that is strongly influenced by temperature, for examination of the health and growth of this species. Embryos can develop with optimal hatching outcomes between 0 and 10 ppt. Higher salinities resulted in an increased osmotic environment internal to the chorion. How this may impact the ontogeny of physiological processes in *H. transpacificus*, specifically those related to salt regulation needs further investigation. Properties of the chorion appear directly affected by salinity which may imply if any tolerance at this stage to environmental salinity exists, it could supported by additional protection of the embryonic membrane. How the chorion forms at fertilization and how the embryo can break free at hatch may be limiting factors for successful transitions between life stages for *H. transpacificus*. This work enhances our understanding of the earliest stages of the life cycle of this species in the context of ecology and conservation.

Supplementary Material

Refer to Web version on PubMed Central for supplementary material.

Acknowledgments

The authors thank Galen Tigan, and Luke Thomas Ellison for providing embryos throughout the breeding season, and Dr. Stuart Meyers for use of microscopes and accessories.

Funding

This work was supported by the Delta Water Quality and Ecosystem Restoration Grant Program from the California Department of Fish and Wildlife, (Proposition 1 Agreement #P1796002 to REC, NAF, T-CH, SMB), the University of California Agricultural Experiment Station (grant 2098-H to NAF), and a National Institute of Environmental Health Sciences (NIEHS) pre-doctoral fellowship (T32 ES007059 to PCM).

REFERENCES

Aanes H, Winata CL, Lin CH, Chen JP, Srinivasan KG, Lee SG, Lim AY, Hajan HS, Collas P, Bourque G (2011) Zebrafish mrna sequencing deciphers novelties in transcriptome dynamics during maternal to zygotic transition. Genome Research 21: 1328–1338 [PubMed: 21555364]

Abrams EW, Mullins MC (2009) Early zebrafish development: It's in the maternal genes. Current Opinion in Genetics & Development 19: 396–403 [PubMed: 19608405]

Alderdice DF (1988) Osmotic and ionic regulation in teleost eggs and larvae In Hoar WS, Randall DJ eds. The physiology of developing fish: Eggs and larvae Vol. 11: Acedemic Press, pp 163–251

Baroux C, Autran D, Gillmor C, Grimanelli D, Grossniklaus U (2008) The maternal to zygotic transition in animals and plants Cold spring harbor symposia on quantitative biology: Cold Spring Harbor Laboratory Press, pp sqb-2008

Baskerville-Bridges B, Lindberg J, Doroshov S (2005) Manual for the intensive culture of delta smelt (hypomesus transpacificus). Report to CALFED Bay-Delta Program

Bennett WA (2005) Critical assessment of the delta smelt population in the san francisco estuary, California. San Francisco Estuary and Watershed Science 3(2)

Brander SM, Jeffries KM, Cole BJ, DeCourten BM, White JW, Hasenbein S, Fangue NA, Connon RE (2016) Transcriptomic changes underlie altered egg protein production and reduced fecundity in an estuarine model fish exposed to bifenthrin. Aquatic Toxicology, 174, 247–260. [PubMed: 26975043]

Brivio MF, Bassi R, Cotelli F (1991) Identification and characterization of the major components of the oncorhynchus mykiss egg chorion. Molecular reproduction and development 28: 85–93 [PubMed: 1847292]

Cherr GN, Clark JR WH (1982) Fine structure of the envelope and micropyles in the eggs of the white sturgeon, acipenser transmontanus richardson: (micropyle/chorion/egg envelopes/sturgeon/egg jelly). Development, Growth & Differentiation 24: 341–352

Cherr GN, Clark WH Jr (1984) Jelly release in the eggs of the white sturgeon, acipenser transmontanus: An enzymatically mediated event. Journal of Experimental Zoology 230: 145–149

Cloern JE, Jassby AD (2012) Drivers of change in estuarine-coastal ecosystems: Discoveries from four decades of study in san francisco bay. Reviews of Geophysics 50(4)

Epel D (1990) The initiation of development at fertilization. Cell differentiation and development 29: 1–12 [PubMed: 2154300]

Finger AJ, Mahardja B, Fisch KM, Benjamin A, Lindberg J, Ellison L,… & May B (2018). A conservation hatchery population of Delta Smelt shows evidence of genetic adaptation to captivity after 9 generations. Journal of Heredity, 109(6), 689–699. [PubMed: 30016452]

Gilkey JC, Jaffe LF, Ridgway EB, Reynolds GT (1978) A free calcium wave traverses the activating egg of the medaka, oryzias latipes. The Journal of Cell Biology 76: 448–466 [PubMed: 10605450]

Hagedom M, Kleinlians FW, Artemov D, Pilatus U (1998) Characterization of a major permeability barrier in the zebrafish embryo. Biology of Reproduction 59: 1240–1250 [PubMed: 9780333]

Hamdoun A, Epel D (2007) Embryo stability and vulnerability in an always changing world. Proceedings of the national academy of sciences 104: 1745–1750

Hasenbein M, Komoroske LM, Connon RE, Geist J, Fangue NA (2013) Turbidity and salinity affect feeding performance and physiological stress in the endangered delta smelt. Integrative and comparative biology 53: 620–634 [PubMed: 23922273]

Hikita T (1958) On the development of long-finned smelt, spirinchus lanceolatus (hikita). Scientific Reports of the Hokkaido Fish Hatchery 13: 39–49

Hobbs J, Moyle PB, Fangue N, Connon RE (2017) Is extinction inevitable for delta smelt and longfin smelt? An opinion and recommendations for recovery. San Francisco Estuary and Watershed Science 15

Kane DA, Kimmel CB (1993) The zebrafish midblastula transition. Development 119: 447–456 [PubMed: 8287796]

Kimmel CB, Ballard WW, Kimmel SR, Ullmann B, Schilling TF (1995) Stages of embryonic development of the zebrafish. Developmental Dynamics 203: 253–310 [PubMed: 8589427]

Komoroske LM, Connon RE, Lindberg J, Cheng B, Castillo G, Hasenbein M, Fangue NA (2014) Ontogeny influences sensitivity to climate change stressors in an endangered fish. Conservation physiology 2

Krogh A, Ussing HH (1937) A note on the permeability of trout eggs to d2o and h2o. Journal of Experimental Biology 14: 35–37

Lee KW, Webb SE, Miller AL (1999) A wave of free cytosolic calcium traverses zebrafish eggs on activation. Developmental biology 214: 168–180 [PubMed: 10491266]

Lee MT, Bonneau AR, Giraldez AJ (2014) Zygotic genome activation during the maternal-to-zygotic transition. Annual review of cell and developmental biology 30: 581–613

Lindberg J, Marzuola C (1993) Delta smelt in a newly-created, flooded island in the sacramento-san joaquin estuary, spring 1993 Report to California Department of Water Resources. Sacramento (CA): California Department of Water Resources

Lindberg JC, Tigan G, Ellison L, Rettinghouse T, Nagel MM, Fisch KM (2013) Aquaculture methods for a genetically managed population of endangered delta smelt. North American Journal of Aquaculture 75: 186–196

Lindeman RE, Pelegri F (2010) Vertebrate maternal-effect genes: Insights into fertilization, early cleavage divisions, and germ cell determinant localization from studies in the zebrafish. Molecular Reproduction and Development 77: 299–313 [PubMed: 19908256]

Machado BE, Podrabsky JE (2007) Salinity tolerance in diapausing embryos of the annual killifish Austrofundulus limnaeus is supported by exceptionally low water and ion permeability. Journal of Comparative Physiology B 177(1): 809.

Mager R, Doroshov S, Van Eenennaam J, Brown R (2003). Early life stages of delta smelt, American Fisheries Society Symposium, American Fisheries Society, pp 169–180

Mangor-Jensen A, Waiwood KG, Peterson RH (1993) Water balance in eggs of striped bass (morone saxatilis). Journal of Fish Biology 43: 345–353

Moyle PB, Lund JR, Bennett WA, Fleenor WE (2010) Habitat variability and complexity in the upper san francisco estuary. San Francisco Estuary and Watershed Science 8(3)

Pelegri F (2003) Maternal factors in zebrafish development. Developmental Dynamics 228: 535–554 [PubMed: 14579391]

Podrabsky J, Riggs C, Romney A, Woll S, Wagner J, Culpepper K, Cleaver T (2017) Embryonic development of the annual killifish *austrofundulus limnaeus*: An emerging model for ecological and evolutionary developmental biology research and instruction. Developmental Dynamics 246: 779–801 [PubMed: 28481428]

Potts W, Rudy P (1969) Water balance in the eggs of the atlantic salmon salmo salar. Journal of Experimental Biology 50: 223–237 [PubMed: 5813345]

Richardson MK, Hanken J, Gooneratne ML, Pieau C, Raynaud A, Selwood L, Wright GM (1997) There is no highly conserved embryonic stage in the vertebrates: Implications for current theories of evolution and development. Anatomy and Embryology 196: 91–106 [PubMed: 9278154]

Riehl R (1996) The ecological significance of the egg envelope in teleosts with special reference to limnic species. Limnologica 26: 183–189

Riehl R, Patzner RA (1998) Minireview: The modes of egg attachment in teleost fishes. Italian Journal of Zoology 65: 415–420

Rizzo E, Sato Y, Barreto B, Godinho H (2002) Adhesiveness and surface patterns of eggs in neotropical freshwater teleosts. Journal of Fish Biology 61: 615–632

Sørensen SR, Butts IAE, Munk P, Tomkiewicz J (2016) Effects of salinity and sea salt type on egg activation, fertilization, buoyancy and early embryology of European eel, Anguilla anguilla. Zygote, 24(1), 121–138. [PubMed: 25707438]

Swanson C (1996) Early development of milkfish: effects of salinity on embryonic and larval metabolism, yolk absorption and growth. Journal of fish Biology, 48(3), 405–421.

Takahashi E, Kawakami Y, Arai K, Yamaha E (2016) Dechorionation of fertilized eggs and embryonic development in arctic rainbow smelt osmerus eperlanus mordax. Fisheries science 82: 639–652

Wang JC (2007) Spawning, early life stages, and early life histories of the osmerids found in the Sacramento-san joaquin delta of California. Bureau of Reclamation, Technical Service Center.

Yamada J (1963) The normal developmental stages of the pond smelt, hypomesus olidus (pallas). 北海道大學水產學部研究彙報= BULLETIN OF THE FACULTY OF FISHERIES HOKKAIDO UNIVERSITY 14: 121–126

Yanagawa H (1978) Embryonic development and fry of the kyuriuo, osmerus eperlanus mordax (mitchill) [salmon and trout]. Bulletin of the Faculty of Fisheries Hokkaido University, 29(3), 195–198.

Zamir E, Kam Z, Yarden A (1997) Transcription-dependent induction of G1 phase during the zebra fish midblastula transition. Molecular and Cellular Biology 17: 529–536. [PubMed: 9001205]

Highlights

- Embryonic development of *H. transpacificus* was described in detail across 22 morphological stages with the maternal to zygotic transition occurring at stage 11, the high blastula stage.
- Embryos had optimal hatching outcomes at salinity treatments between 0.4 and 10 ppt.
- At higher salinity treatments, embryos had increased intrachorionic osmolalities and reduced yolk masses.
- Lower salinity treatments resulted in altered rates of egg activation, a critical process which occurs prior to fertilization.

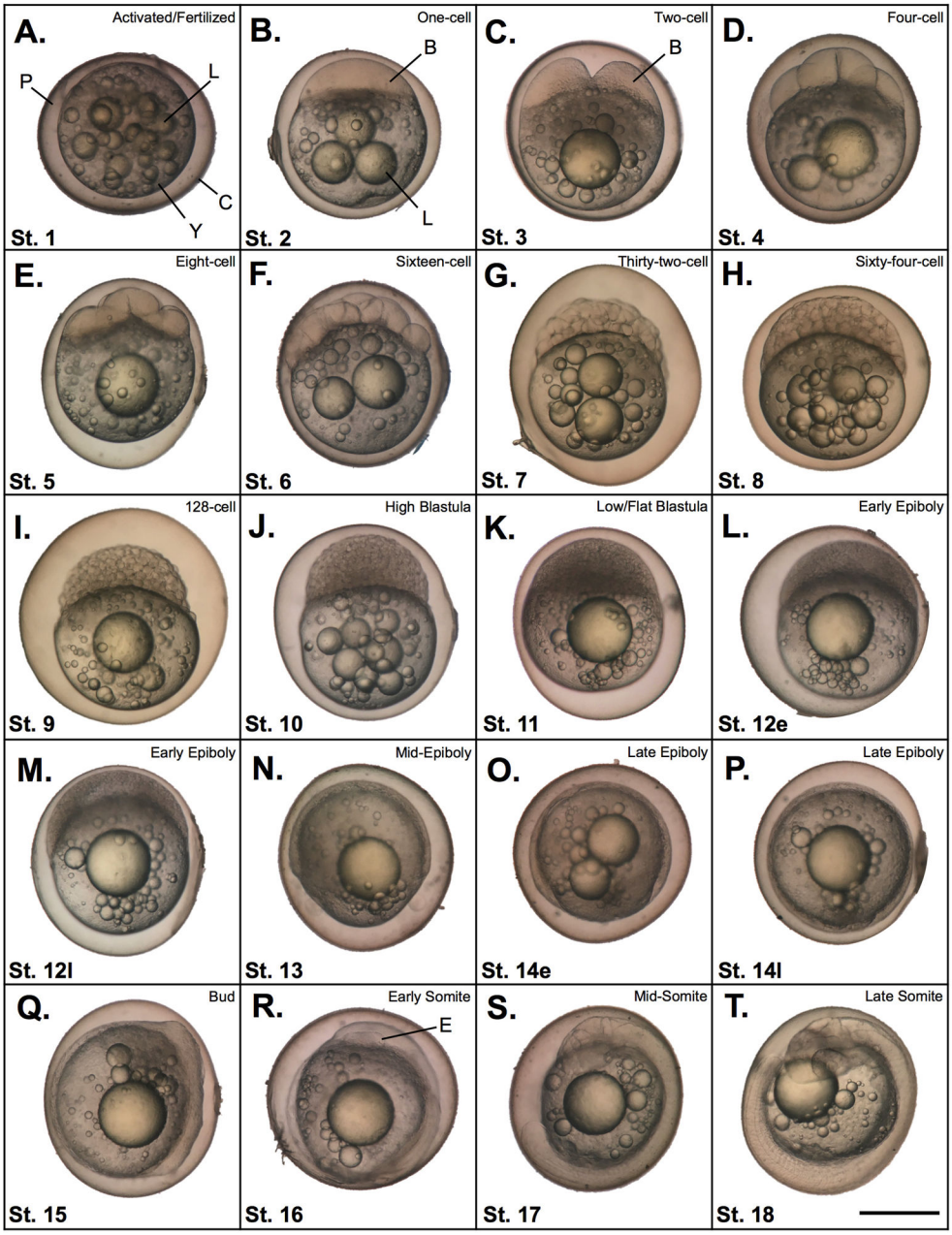

Figure 1: Morphological stages of *H. transpacificus* embryonic development from fertilization through somitogenesis.

In each panel (A-T), the stage number is at the bottom left and the stage name is at the top right. C = Chorion, P = perivitelline space, Y = yolk, L = lipid droplet, B = Blastomere, E = Eye. Scale bar at the bottom right represents 500 μm.

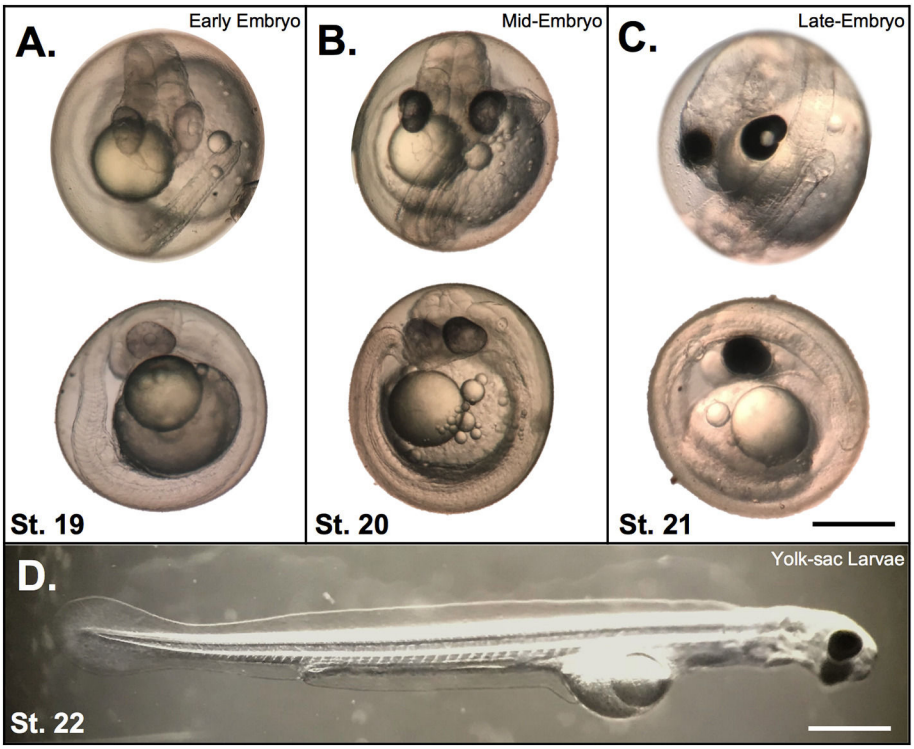

Figure 2: Morphological stages of *H. transpacificus* embryonic development from early embryo to yolk-sac larvae.

In each panel (A-D), The upper image shows the morphology of the dorsal aspect of the embryonic head and the lower image shows the morphology of the lateral aspect of the embryonic head. The stage number is at the bottom left and the stage name is at the top right. The black scale bar is representative for embryo images (A-C), and the white scale bar is representative only of the larva (D); both are 500 μm.

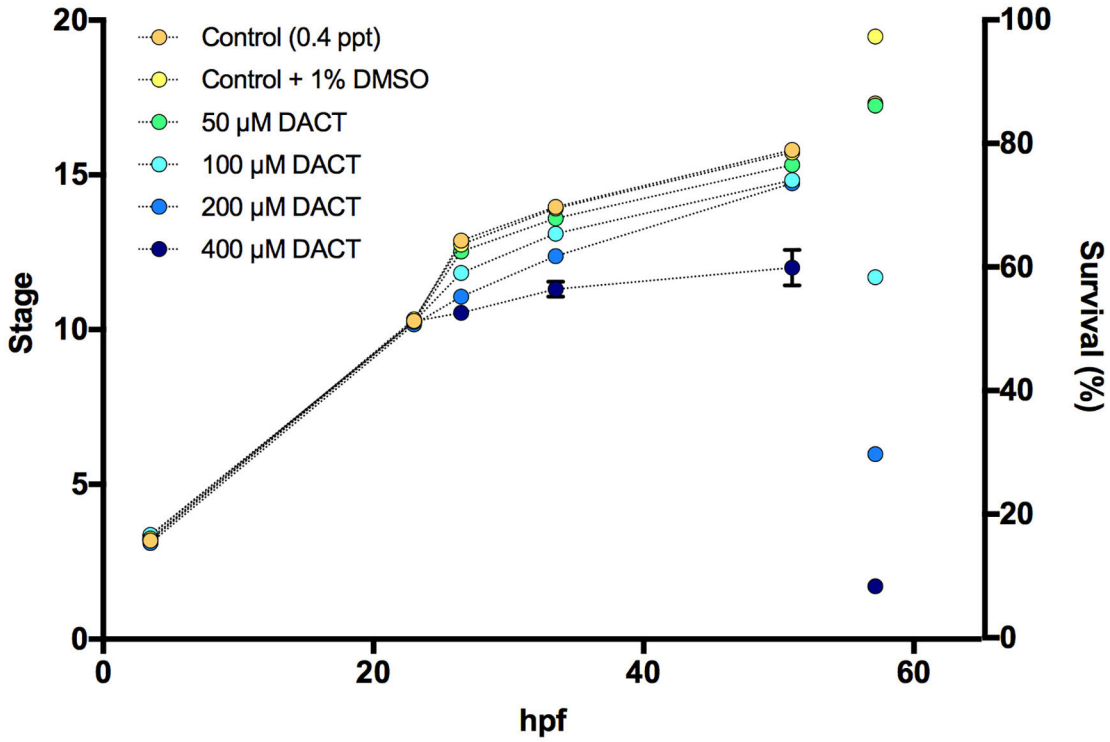

Figure 3: Midblastula transition in *H. transpacificus*.

Upon fertilization, embryos incubated at increasing concentrations of actinomycin-D showed stalled development at the high blastula (stage 11) and subsequent high mortality. Plot depicts mean stage count (left y-axis) ± SEM for each time point (hpf) and for each treatment concentration combined with survival counts (percent; right y-axis).

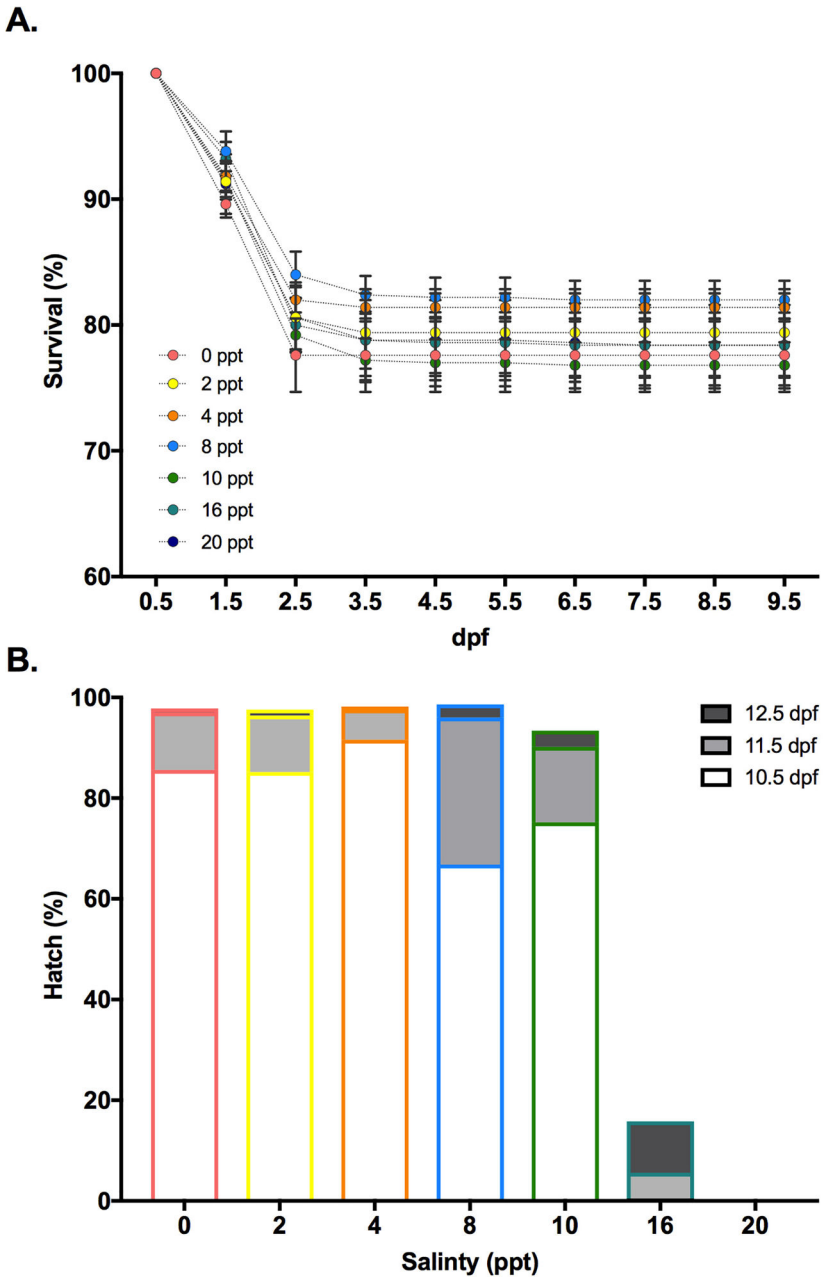

Figure 4: Embryonic survival and hatching of *H. transpacificus* incubated at alternative salinities.

A) Mean embryo survival (percent) ± SEM for each treatment salinity across 9 days of 24 h observations. B) Stacked histogram shows cumulative as well as the percent hatch per day (10.5, 11.5, and 12.5 dpf) for embryos incubated at each salinity.

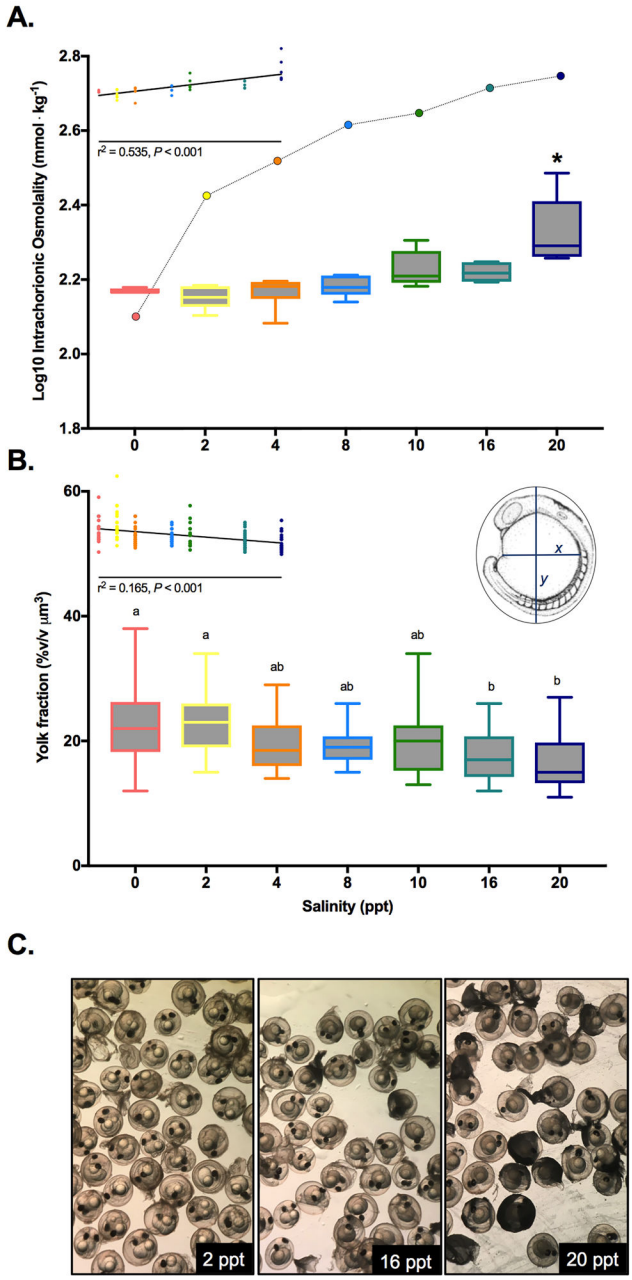

Figure 5: Intrachorionic osmolality and yolk fraction of *H. transpacificus* embryos incubated at alternative salinities.

A) Log 10 transformed mean osmolality (mmol · kg^{-1}) and inter-quartile range with minimum and maximum measurements for each treatment group with. The dotted line represents the measure of osmotic pressure for each salinity treatment. The asterisk above the 20.0 ppt data represent significant difference from all other treatment groups ($P < 0.05$). The inset image in the upper left represents a linear regression with a significant positive trend with increasing salinities. B) Mean yolk fraction (%) and inter-quartile range with minimum and maximum measurements for each treatment group. Different letters indicate significant differences between treatments ($P < 0.05$). The inset image in the upper left

represents a linear regression showing a significant positive trend with increasing salinities (r^2 = .4504, $P < 0.01$). C) Photographs of embryos under the microscope (20X) representing the physical characteristics of chorions at different salinities. The leftmost picture is at a treatment of 2.0 ppt and is representative of 0.4, 4.0, 8.0, and 10.0 ppt treated embryos. The center picture is at 16.0 ppt salinity and the rightmost image is at 20.0 ppt.

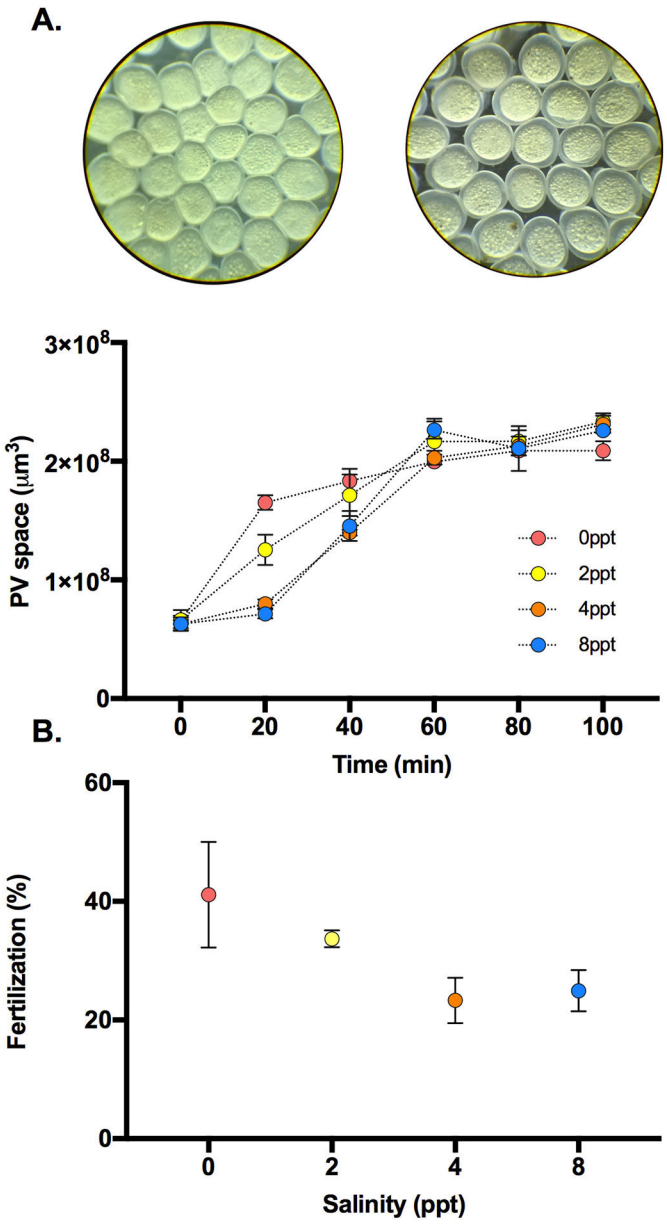

Figure 6: Egg activation and fertilization of *H. transpacificus* embryos at alternative salinities.
A) Images at top show perivitelline space expansion associated with egg activation in unfertilized eggs extruded into 0.4 ppt water after 10 min (left) and 1 h (right). Mean volume perivitelline space (μm^3) ± SEM in unfertilized eggs exposed to treatment salinities over time. B) Mean fertilization percent ± SEM in eggs exposed to sperm under different salinities ($P > 0.05$).

Table 1:

Stages of embryonic development across conserved morphological periods of *H. transpacificus*.

Period	Stage #	Stage Name	Timeline (16°C)	
			hpf	dpf
Pre-fertilization	0	Unfertilized egg	-	-
Zygote	1	Activated/Fertilized	0-1	0
	2	One-cell	1-2.5	0
Cleavage	3	Two-cell	2.5-4	0
	4	Four-cell	4-5	0
	5	Eight-cell	5-6	0
	6	Sixteen-cell	6-7	0
	7	Thirty-two-cell	7-8	0
	8	Sixty-four-cell	8-10	0
	9	128-cell	11-14	0
Blastula	10	High Blastula	14-22	0
	11	Low/Flat Blastula	22-26	1
Gastrula	12	Early Epiboly	26-29	1
	13	Mid-Epiboly	29-32	1
	14	Late Epiboly	32-37	1
	15	Bud	37-48	1
Segmentation	16	Early Somite	48-56	2
	17	Mid-Somite	56-77	2
	18	Late Somite	77-96	3-4
Pharyngula	19	Early Embryo	96-120	4-5
	20	Mid-Embryo	120-150	5-6.5
	21	Late Embryo	150+	6.5-10
Larvae	22	Yolk-sac Larvae	240-288	10-12

hpf = hours post-fertilization; dpf = days post-fertilization.